Diffusion and perfusion MR parameters to assess preoperative short course radiotherapy response in locally advanced rectal cancer: a comparative explorative study among parameters derived from standardized index of shape DCE-MRI, intravoxel incoherent motion and diffusion kurtosis imaging

Antonella Petrillo[1]; Roberta Fusco[1]; Mario Sansone[2]; Vincenza Granata[1]; Robert Grimm[3]; Daniela Rega[4]; Paolo Delrio[4]; Francesco Bianco[4]; Massimiliano Di Marzo[4]; Fabiana Tatangelo[5]; Antonio Avallone[6]; Biagio Pecori[7]

[1] Division of Radiology, Istituto Nazionale Tumori (IRCCS) Fondazione G. Pascale, Naples, Italy

[2] Division of Information Technology and Electrical Engineering (DIETI), Naples, Italy

[3] Siemens Healthineers, Erlangen, Germany

[4] Division of Gastrointestinal Surgical Oncology, Istituto Nazionale Tumori (IRCCS), Fondazione G. Pascale, Naples, Italy

[5] Division of Diagnostic Pathology, Istituto Nazionale Tumori (IRCCS), Fondazione G. Pascale, Naples, Italy

[6] Division of Gastrointestinal Medical Oncology, Istituto Nazionale Tumori (IRCCS), Fondazione G. Pascale, Naples, Italy

[7] Divion of Radiotherapy, Istituto Nazionale Tumori (IRCCS), Fondazione G. Pascale, Naples, Italy

Abstract

Purpose

To assess preoperative Short Course Radiotherapy (SCR) tumor response in locally advanced rectal cancer (LARC) by means of parameters derived from Standardized Index of Shape (SIS) dynamic contrast-enhanced (DCE) MRI, Apparent Diffusion Coefficient (ADC), Intravoxel Incoherent Motion and Diffusion Kurtosis Imaging derived parameters by diffusion-weighted (DW) MRI.

Materials and methods

34 patients with LARC were enrolled for the study. The participants underwent MRI before and after SCR, followed by delayed surgery, retrospectively. SIS, ADC, tissue diffusion (Dt), pseudo-diffusion (Dp), perfusion fraction (fp), mean diffusivity (MD), and mean diffusional kurtosis (MK) were calculated for each patient. After surgery, the pathological TNM and tumor regression grade (TRG) were estimated. For each parameter, percentage changes between the values before and after SCR were evaluated. Non-parametric sample tests and receiver operating characteristic curve (ROC) analysis were performed.

Results

15 patients were classified as responders (TRG ≤ 2) and 19 as non-responders (TRG > 3). Seven patients had TRG 1 (pathological complete response, pCR). A Mann-Whitney test showed statistically significant differences only for the percentage change in SIS median values between responder and non-responder patients and between complete and incomplete pathological response (p value << 0.001). The best result to differentiate responders from non-responders and to assess complete pathological response was achieved by SIS with an accuracy of 89% and an area under the ROC curve of 0.95 and 0.88, respectively. A high accuracy (74%) was also obtained by perfusion fraction to detect pathological complete response after SCR with an area under the ROC of 0.70.

Conclusion

SIS is a promising DCE-MRI angiogenic biomarker for assessing preoperative treatment response after SCR with delayed surgery and it permits to discriminate pCR allowing to direct surgery for tailored and conservative treatment. However, parameters derived from IVIM and DKI reflect tissue response changes and could be used to assess pathological response in LARC after SCR.

Introduction

Total mesorectal excision combined with preoperative radiation therapy and chemotherapy (pCRT) is the current standard procedure for locally advanced rectal cancer (LARC) [1–3]. Long-course CRT has been extensively applied and results from this approach have been encouraging in terms of local control with a high percentage of tumor regression up to a significant complete response rate [1–3]. However, Short Course Radiotherapy (SCR) is known to be a valuable therapeutic option in patients with LARC. A recent meta-analysis [4] reported that SCR with immediate surgery is as effective as long CRT with deferred surgery in terms of overall and disease-free survival rates, local and distant control, and toxicity. Also, Short Course Radiotherapy with Delayed Surgery (SCRDS) (after 4~8 weeks), an optional therapy prescribed for patients with locally advanced tumors who are not fit for CRT, leads to similar results in terms of the percentage of patients with a negative margin resection and satisfactory results with regard to the downstaging and pathological response rate compared to traditional preoperative CRT [5–13].

The use of new imaging modalities to make individual assessments of therapy response could be of great clinical value to enable subsequent strategies to be tailored to each patient. Such strategies range from a tailored surgical approach, to administering an adjuvant regimen, or even a wait-and-see policy without surgery for patients with high surgical risks [14, 15].

A positive tumor response will not necessarily correspond to a significant tumor size reduction using morphological MRI [16]; it is difficult to differentiate between necrosis, fibrotic tissue, and viable residual tumor tissue within the treated areas [16, 17]. Several studies have focused on the potential added benefit of functional quantitative parameters derived from MR images [17–20]. Dynamic contrast-enhanced MRI (DCE-MRI) has proven promising for the detection of residual tumor following pre-surgery CRT [17–21]. Earlier studies investigated the functional parameters derived from DCE-MRI data in rectal cancer [18–21] such as the Standardized Index of Shape proposed by Petrillo et al. [18] as a simple semi-quantitative parameter capable of differentiating pathological significant and complete response after CRT in LARC and after SCRDS [22]. Moreover, in various oncology fields, researchers have recommended the use of diffusion-weighted imaging (DWI) to assess treatment response [23–30]. DWI provides functional information on tissue microstructure by evaluating water proton mobility differences [23, 24]. Water diffusion characteristics depend on cell density, vascularity, viscosity of the extracellular fluid and cell membrane integrity. By quantifying these properties by means of the individual apparent diffusion coefficient (ADC), using a mono-exponential model to analyze DWI data, it can be employed as an imaging biomarker to detect biological tumor changes and to monitor and predict treatment response [25, 26]. Moreover, using a bi-exponential model to analyze DWI data, we can obtain information on both diffusion and perfusion tissue properties derived from Intravoxel Incoherent motion method (IVIM): the pure tissue coefficient (D) that describes macroscopic motion of water in the cellular interstitial space, the pseudo-diffusion coefficient (Dp) that describes the microscopic motion of blood in the vessels, and the perfusion fraction (fp) that describes the proportion of two different motions [27–30].

Also, the conventional DWI model is based on the assumption that water diffusion within a voxel has a single component and exhibits Gaussian behavior where water molecules diffuse with no restrictions [31]. However, due to the presence of microstructures (i.e., two tissue types or components within one voxel, organelles, and cell membranes), random motion or diffusion of thermally agitated water molecules within biological tissue exhibits non-Gaussian behavior [32]. In 2005, Jensen and colleagues proposed a non-Gaussian diffusion model entitled Diffusion Kurtosis Imaging (DKI) [32]. This model includes the kurtosis coefficient (K), which measures the deviation of tissue diffusion from a Gaussian model, and the diffusion coefficient (D) with the non-Gaussian bias correction.

The aim of this study is to determine the diagnostic performance of MR imaging for the assessment of tumor response after SCRDS in patients with LARC using Standardized Index of Shape (SIS) obtained from DCE-MRI, using parameters derived from ADC, IVIM, and DKI obtained from DW-MRI.

Material and methods

Patient selection

34 patients with a median age of 67 years (range 48–83 years) who refused or were considered unfit for chemo radiation and planned for neoadjuvant Short Course Radiotherapy, were evaluated in this retrospective study, conducted from May 2011 to December 2016.

Patient characteristics are described in Table 1.

All patients had a biopsy-proven rectal adenocarcinoma. Endorectal ultrasonography, MRI of pelvis and Computed Tomography (CT) scan of the chest, abdomen, and pelvis were used as staging examinations. Patients had T2-T3 rectal cancer with and without local lymph node involvement. Patients staged T2 without lymph node involvement were included only if the tumor was located less than 5 cm from the anal verge. Exclusion criteria were:

Characteristics	All patients n = 34 (%)	TRG 1–2 n = 15	TRG 3–4 n = 19	p*
Gender				> 0.05
Male/Female	26 (76.5) 8 (23.5)	10/5	16/3	
Median age (range)	67 (48–83)	69 (48–78)	68 (48–76)	
Gunderson Risk				> 0.05
Intermediate: T3N0, T2N1	8 (23.5)	3	5	
Moderately high: T2N2, T3N1, T4N0	17 (50.0)	7	10	
High: T3N2	9 (26.5)	5	4	
Distance from the anal verge				> 0.05
≤ 5 cm	14 (41.2)	6	8	
> 5 cm	20 (58.8)	9	11	
Circumferential resection margin				> 0.05
> 2 mm	15 (44.1)	6	9	
≤ 2 mm	13 (38.2)	6	7	
≤ 1 mm	5 (14.7)	2	3	
Not measurable	1 (2.9)	0	1	

Table 1:
Patient characteristics and histopathological findings.

inability to give informed consent, previous rectal surgery, and contraindications to MRI or to the administration of MR contrast media. Patients were included in the study in accordance with the approved guidelines of the Ethical Committee of the National Cancer Institute of Naples and gave their written informed consent.

Radiotherapy

All patients underwent dose-planning CT in prone position. After an online CT virtual simulation, CT datasets were transferred to a dedicated treatment planning system through a DICOM network and an individualized clinical target volume (CTV) was calculated, including the gross tumor volume with margins (2–3 cm depending on tumor position, identified by MRI imaging), the mesorectum, and regional lymph nodes depending on tumor location. We contoured the small bowel, the femoral heads, and the bladder as critical organs on all CT slices for every patient, and we evaluated the relative dose-volume histogram on the treatment planning console. Three-dimensional plans for 3D or Intensity-Modulated Radiation Therapy (IMRT) radiotherapy were generated for dual-energy, 6–20 MV X-rays, (Clinac 2100, Varian Medical Systems, Palo Alto, CA, USA), or 6–15 MV X-ray linear accelerator (Elekta

Agility, Elekta Instrument AB Stockholm, Sweden) both equipped with multileaf collimators (MLC). Patients were scheduled using a 3-field or IMRT treatment arrangement to include the planning target volume within the 95% isodose. A dose of 25 Gy in 5 fractions over 1 week was prescribed to the ICRU 62 intersection point.

MRI data acquisitions

Each patient underwent MR studies before and after SCR: baseline, on average 23.8 days before starting radiotherapy and delayed, on average 61.0 days after the end of SCR. MR imaging was performed with a 1.5T scanner (MAGNETOM Symphony, Siemens Healthcare, Erlangen, Germany) equipped with a phased-array body coil. Patients were placed in a supine, head-first position. Mild rectal lumen distension was achieved with 60–90 mL of undiluted Ferumoxsil (Lumirem, Guerbet, Roissy, France) suspension introduced per rectum. Pre-contrast coronal T1w 2D turbo spin-echo (TSE) images and sagittal and axial T2w 2D turbo spin-echo images of the pelvis were obtained. Axial DWIs were then acquired (spin-echo diffusion-weighted echo-planar imaging (SE-DW-EPI) at seven b-values of 0, 50, 100, 150, 300, 600, 800 s/mm^2. Subsequently, axial, dynamic, contrast-enhanced T1w, FLASH 3D gradient-echo images were acquired. We obtained one sequence before and ten sequences, with no delay, after IV injection of 0.1 mmol/kg of a positive, gadolinium-based para-magnetic contrast medium (Gd-DOTA, Dotarem, Guerbet, Roissy, France). The contrast medium was injected using Spectris Solaris® EP MR (MEDRAD Inc., Indianola, PA, USA), with a flow rate of 2 mL/s, followed by a 10-mL saline flush at the same rate. Temporal resolution was 0.58 minutes, corresponding to 35 seconds (as reported in Table 2). Sagittal, axial, and coronal post-contrast T1w 2D turbo spin-echo images, with and without fat saturation, were then obtained (Table 2). Axial T1w pre- and post-contrast sequences were acquired at the same position as the T2w sequence. MRI total acquisition time was around 40 minutes. Patients did not receive bowel preparation, antispasmodic medication, or rectal distention before any of the MR examinations.

MR image data analysis

Image assessment was performed in a single reading session for each patient based on the consensus of two gastro-intestinal radiologists with 25 years and 10 years of experience in reading pelvic MR images.

To take into account tumor heterogeneity, based on pre-contrast T1-weighted images using the T2-weighted images as a guide [33], the radiologists manually drew regions of interest (ROI) along the contours of the tumor to obtain the DCE-MR volume of interest (VOI) for each study, covering the whole lesion with the exclusion of peripheral

Sequence	Orientation	TR/TE/FA (ms/ms/deg.)	FOV (mm x mm)	Pixel Spacing	ST/Gap (mm/mm)
T1w 2D TSE	Coronal	499/13/150	450 x 450	0.87 x 0.87	3/0
T2w 2D TSE	Sagittal	4820/98/150	250 x 250	0.78 x 0.78	3/0
T2w 2D TSE	Axial	3970/98/150	250 x 250	0.78 x 0.78	3/0
SE-DW-EPI	Axial	2700/83	270 x 230	1.70 x 1.70	4/0
T1w FLASH 3D, pre-contrast	Axial	9.8/4.76/25	330 x 247	0.59 x 0.59	3/0
T1w FLASH 3D, post-contrast	Axial	9.8/4.76/25	330 x 247	0.59 x 0.59	3/0
T1w 2D TSE	Sagittal	538/13/150	250 x 250	0.48 x 0.48	3/0
T1w 2D TSE	Coronal	538/13/150	250 x 250	0.48 x 0.48	3/0
T1w 2D TSE	Axial	450/12/150	270 x 236	0.52 x 0.52	3/0

Table 2:
Pulse sequence parameters in MR studies.

Abbreviations: TR = Repetition Time, TE = Echo Time, FOV = Field of View, FA = Flip Angle, ST = Slice Thickness, TF = Turbo Factor, AT = Acquisition Time
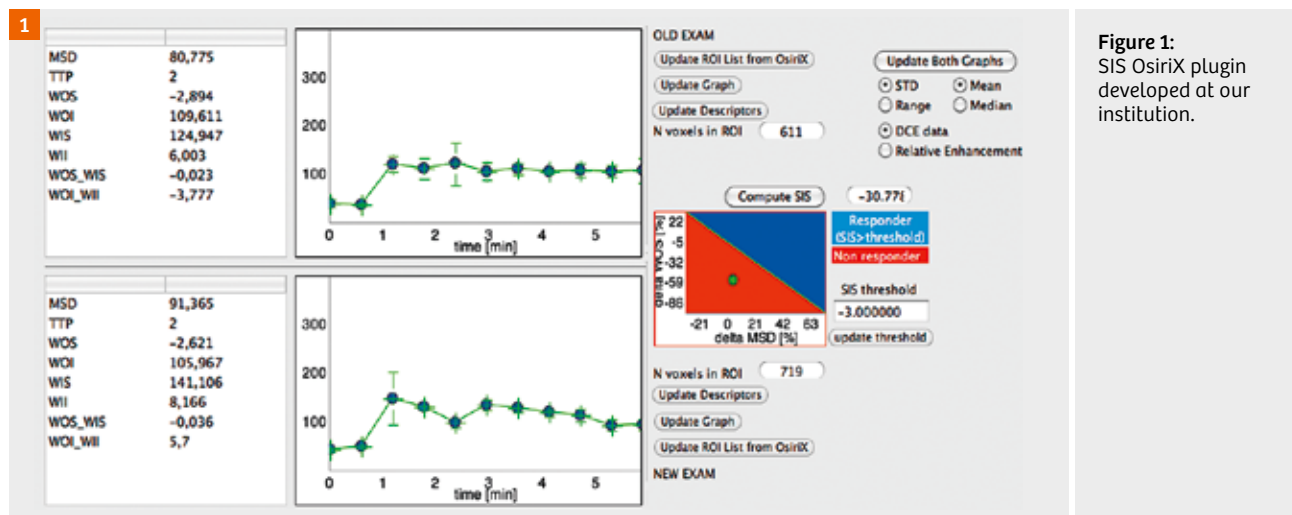

Figure 1:
SIS OsiriX plugin developed at our institution.

fat, artefacts, and blood vessels. Also, for DW-MRI, based on DWI with the highest b-value, the radiologists, manually drew regions of interest (ROI) along the contours of the tumor to obtain the DW-MR volume of interest (VOI) for each study.

For each MR descriptor, the percentage change of the mean value on the VOI between pre and post treatment was calculated as ΔX = (Xpre – Xpost) / Xpre (X is the generic shape descriptor).

No image registration was applied to the data we acquired. We took care to exclude from the analysis the slices where motion artifacts were visible. Moreover, a volumetric analysis was performed for each parameter thus minimizing errors due to voxel misalignments.

DCE-MRI features
In order to perform SIS analysis, the authors developed an OsiriX plugin (Fig. 1) [34]. Considering the segmented VOI, the maximum signal difference (MSD) and wash out slope (WOS) were calculated as reported in [35]. For the SIS analysis, we then evaluated the percentage change of MSD [$\Delta MSD = (MSD_1 - MSD_2) / MSD_1 \times 100$], of WOS [$\Delta WOS = (WOS_1 - WOS_2) / WOS_1 \times 100$] and of the two combined as described in a previous paper [18].

DWI features
For each voxel, 9 features were extracted from DWI data using the mono-exponential model, the Diffusion Kurtosis Imaging model, and Intra Voxel Incoherent Motion imaging using a conventional biexponential fitting method (CBFM).

DWI signal decay is most commonly analyzed using the monoexponential model [23, 24]:

Equation 1

$$ADC = \frac{\ln\left(\frac{S_0}{S_b}\right)}{b}$$

where S_b is the MRI signal intensity with diffusion weighting b, S_0 is the non-diffusion-weighted signal intensity, and ADC is the apparent diffusion coefficient.

For a voxel with a large vascular fraction, the MRI data decay can deviate from a monoexponential form, in particular showing rapid decay in the range of low b values generated by the IVIM effect [23, 24]. Thus, in addition to the monoexponential model, a conventional biexponential model was used to estimate the IVIM-related parameters of pseudo-diffusivity (Dp indicated also with D*), perfusion fraction (fp), and tissue diffusivity (Dt):

Equation 2

$$\frac{S_0}{S_b} = f_p \cdot \exp(-b \cdot D_p) + (1 - f_p) \cdot \exp(-b \cdot D_t)$$

Moreover, Diffusion Kurtosis imaging was included in the analysis in order to obtain the final fitted images (Mean of Diffusion Coefficient (MD) and mean of Diffusional Kurtosis (MK)).

Multi-b DW images were obtained through voxel-by-voxel fitting using the diffusion kurtosis signal decay equation (3) by applying a two-variable linear least squares algorithm as used in a previous study [32]:

Equation 3

$$S(b) = S_0 \exp\left(-b \cdot D + \frac{1}{6} b^2 \cdot D^2 \cdot K\right)$$

In this equation, D is a corrected diffusion coefficient; and K is the excess diffusion kurtosis coefficient. K describes the degree of deviation of molecular motion from the perfect Gaussian distribution. When K is equal to 0, equation (3) evolves into a conventional monoexponential equation (1):

The difference between D and ADC is that D is a corrected form of ADC for use in non-Gaussian circumstances.

The parameters of conventional DWI (ADC), IVIM (fp, Dt, Dp), and DKI (MK and MD) were obtained from the multi-b DWI data with all measured b values using the prototype post-processing software Body Diffusion Toolbox[1] (Algorithm 0 for IVIM fitting) produced by Siemens Healthcare, Erlangen, Germany.

[1] WIP, the product is currently under development and is not for sale in the US and in other countries. Its future availability cannot be ensured.
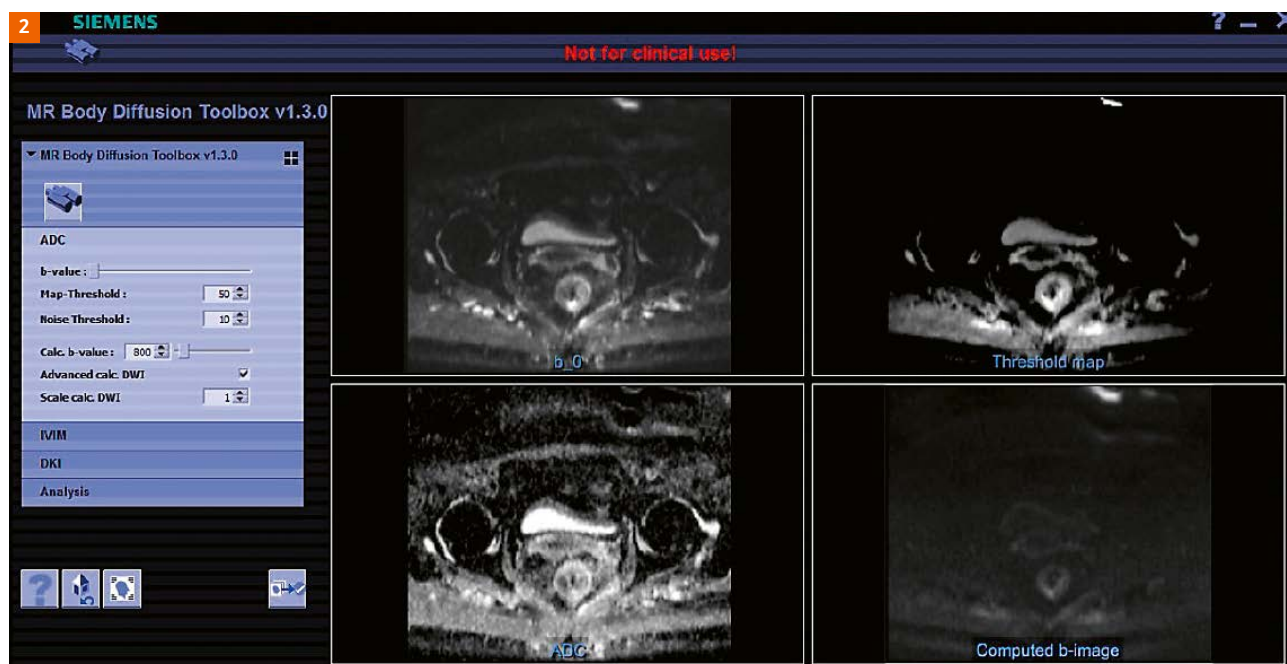

Figure 2:
Siemens Healthineers MR Body Diffusion Toolbox[1] interface.

Surgery

Surgery was performed, on average, 70.0 days after the end of radiotherapy. Based on the results of restaging and downsizing, sphincter-saving surgery was considered for all patients without clear sphincter involvement before treatment and local excision was considered for patients with a significant clinical response. The planned operation was discussed with the patients and a specific informed consent was obtained. A rectal resection with total mesorectal excision and bilateral nerve sparing, where possible, was the standard approach. In distal cancers an ultra-low anterior resection with colo-anal manual anastomosis or, in the case of sphincter involvement, an abdomino-perineal resection were performed. All patients receiving an anastomosis underwent construction of a protecting ileostomy.

Evaluation of pathologic response

Details of how the pathologic response assessment was performed have been described [36, 37]. In brief, surgical specimens containing the tumor were evaluated and scored according to tumor regression grade (TRG), as proposed by Mandard et al. [37], by an expert pathologist who was not aware of the MRI findings. A score of TRG 1 means a complete response with absence of residual cancer and fibrosis extending through the wall. TRG 2 is defined as the presence of residual cancer cells scattered through the fibrosis. TRG 3 corresponds to an increased number of residual cancer cells, with predominant fibrosis. TRG 4 indicates residual cancer outgrowing fibrosis. TRG 5 is the absence of regressive changes. Patients with a TRG 1 or 2 score were considered as responders, whereas the remaining patients (TRG 3, 4, or 5) were classified as non-responders. Patients with TRG 1 were considered as having achieved pathological complete response while patients with TRG 2–5 were considered as having incomplete pathological response [18].

Statistical analysis

A Mann-Whitney non-parametric test was performed to assess statistically significant differences between responder and non-responder patients and between pathological complete responders and incomplete responders. Receiver Operating Characteristic (ROC) curves were also used to evaluate the diagnostic performance for each parameter. The Area Under ROC Curve (AUC) was calculated and optimal thresholds were obtained by maximizing the Youden index. Sensitivity, specificity, positive predictive value (PPV), negative predictive value (NPV), and accuracy were performed considering optimal cut-off values.

A P value < 0.05 was considered significant for all tests. All analyses were performed using the Statistics Toolbox produced by Matlab R2007a (The Math-Works, Natick, MA, USA).

Results

All patients in our series had rectal adenocarcinomas. Three patients were pathologically classified as T0, 6 as T1, 20 as T2, 5 as T3. There were 7 patients with a TRG 1, 8 with a TRG 2, 11 with a TRG 3, 8 with a TRG 4, and none with a TRG 5. Therefore, 15 patients were classified as responders and 19 as non-responders according to TRG. Seven patients had pathological complete response. The results of the parameters were reported in terms of percentage changes between pre and post therapy (symbol Δ).

A Mann-Whitney test showed statistically significant differences exclusively for SIS percentage change median values between responder and non-responder patients and between complete and incomplete pathological response (p value << 0.001, Fig. 3). Figure 3 shows the boxplots for SIS in discrimination of responders from non-responders (3A) and in discrimination of complete from incomplete response (3B). Figure 4 shows the boxplots for each diffusion parameter between responders and non-responders and Figure 5 between complete and incomplete responders. Table 3 shows the change in SIS and diffusion parameters to differentiate the responders and the non-responders group and Table 4 to discriminate complete pathological response from incomplete pathological response. Results were statistically significant for every parameter (Fisher test p < 0.01). The best parameter to discriminate responders from non-responders was SIS (sensitivity 94%, specificity 84%, AUC = 0.95, cut-off value = -7.8%). For IVIM-derived parameters the best results to discriminate responders from non-responders were obtained with Dt (sensitivity 75%, specificity 74%, AUC = 0.63, cut-off value = 25.59%). SIS obtained the best diagnostic performance also to discriminate pCR (sensitivity 86%, specificity 89%, AUC = 0.88, cut-off value = 68.2%). A high AUC (0.70) was also obtained by fp to detect pathological complete response after SCR with a cut-off value = 15.32%.

Figure 6A shows ROC analysis for ΔSIS and the change in parameters derived from DW-MRI to discriminate responders from non-responders while Figure 6B shows ROC analysis for ΔSIS and change in diffusion parameters to detect complete pathological response versus incomplete pathological response.

Discussion and conclusions

In recent years, there has been growing interest in functional imaging modalities to increase diagnostic accuracy for therapy response assessment. These imaging modalities reflect the microstructural and metabolic proprieties of a tumor, allowing the evaluation of treatment-induced changes before morphological changes become apparent. DCE-MRI and DWI have emerged as

Figure 3:
Boxplots of SIS to discriminate responders from non-responders and to detect complete pathological response (pCR).

Figure 4:
Boxplots of diffusion parameters to discriminate responders from non-responders.
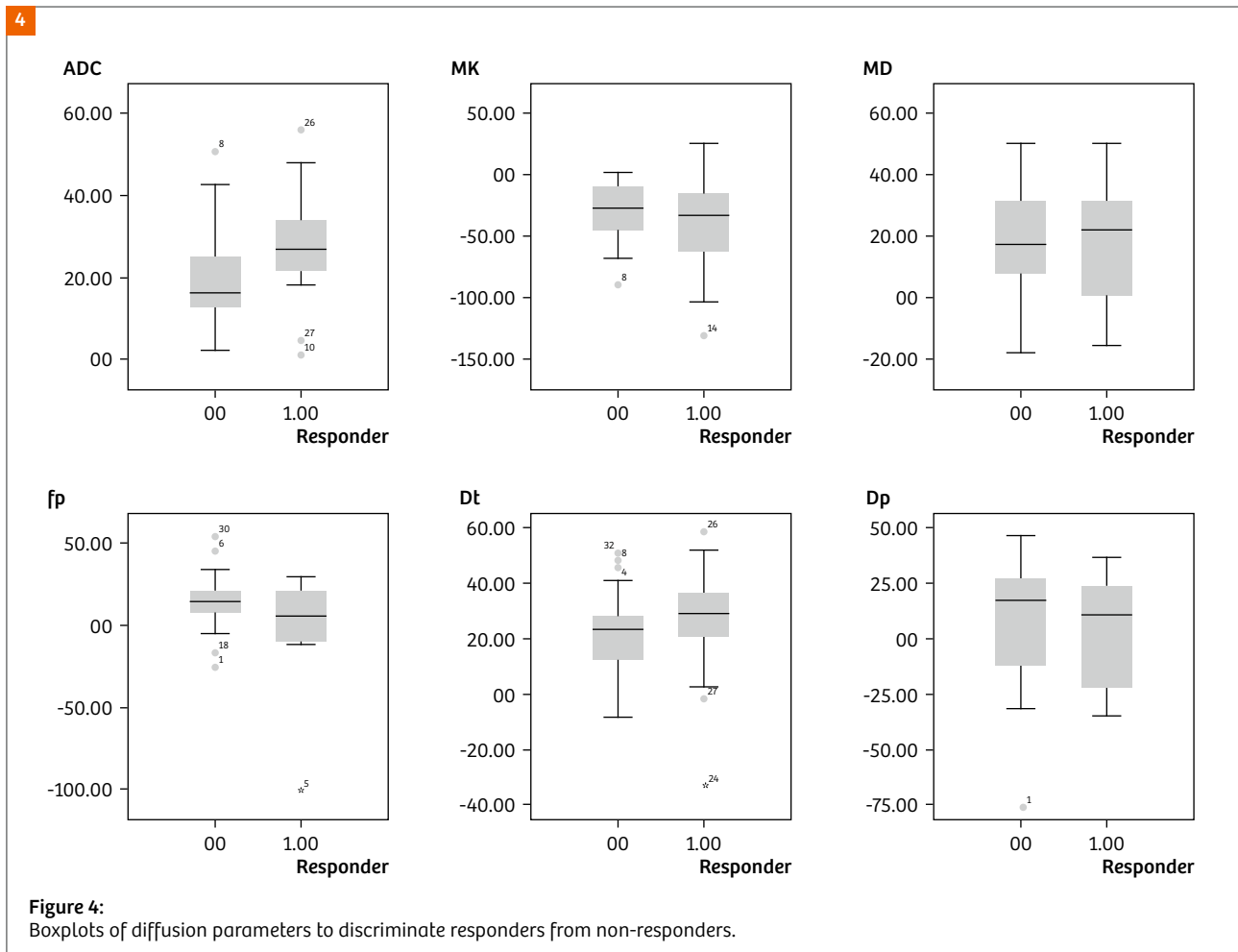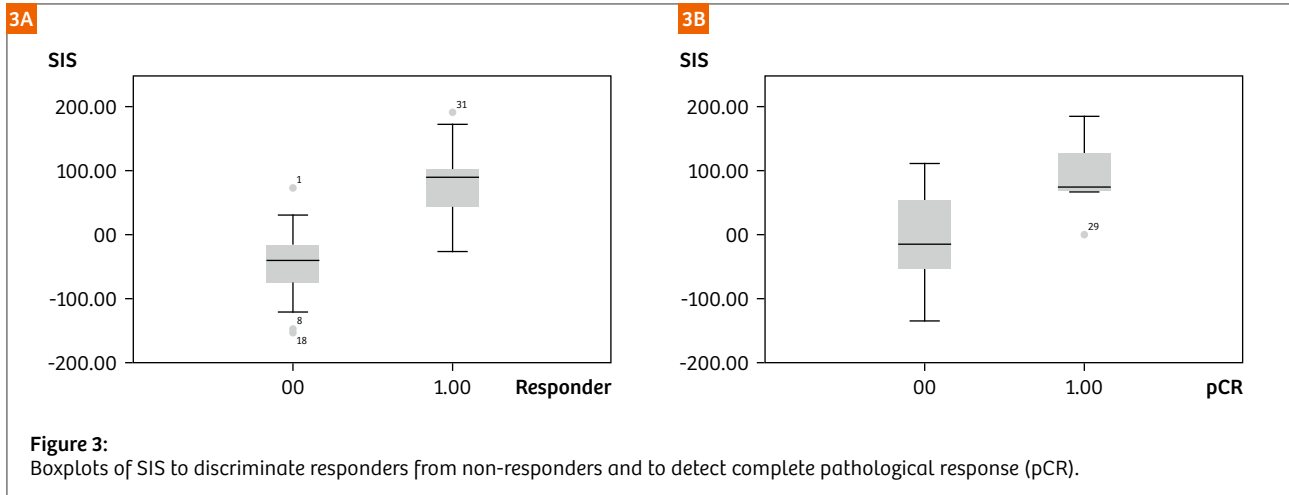
powerful tools for predicting and assessing neoadjuvant therapy response for rectal cancer. In fact, DCE-MR and DW-MR imaging after preoperative CRT were shown to be more valuable than morphologic MR imaging in recognizing significant and pathological complete response and in identifying residual tumor.

The objective of this study is to determine the diagnostic performance of DCE and DW imaging for the assessment of tumor response after SCRDS in patients with LARC, comparing Standardized Index of Shape (SIS) obtained by DCE-MRI and using ADC, parameters derived from Intravoxel Incoherent Motion and DKI obtained by DW-MRI. To the best of our knowledge, there are no studies in the literature focusing on a comparison of parameters derived from DCE-MRI, IVIM, and DKI to assess therapy response in locally advanced rectal cancer after SCRDS.

There are many studies that evaluate the single modality, DCE and DWI, in preoperative long CRT assessment [18–21, 38–40]. In our previous studies [18] we demonstrated the ability of DCE-MRI using the Standardized Index of Shape

to discriminate responder from non-responder patients and complete pathological tumor response after CRT in LARC with a high degree of accuracy, also when compared to FDG-PET examination [41]. Several studies have already demonstrated the role of diffusion-weighted imaging in LARC for early and late assessment of therapy response [38–40] and several studies have also evaluated the use of IVIM in elaborating DW-data in different types of tumors [27–30, 42]. Moreover, there are some studies that aim to assess tumor response after SCR using metabolic change evaluations revealed by FDG-PET with contrasting results [43–46]. Two studies [45, 46] have analyzed the responses to SCR in LARC, documenting no significant metabolic responses to SCR. However, Pecori et al. [44] demonstrated that, in the course of SCR, it is possible to estimate the probability of pathological tumor responses on the basis of a logistic regression analysis of PET/CT parameters derived from three sequential studies. In another of our studies [19], we assessed parameters derived from SIS and IVIM in LARC after SCRDS, demonstrating that SIS obtained the best parameter for discriminating responders

Figure 5:
Boxplots of diffusion parameters to detect complete pathological response (pCR).
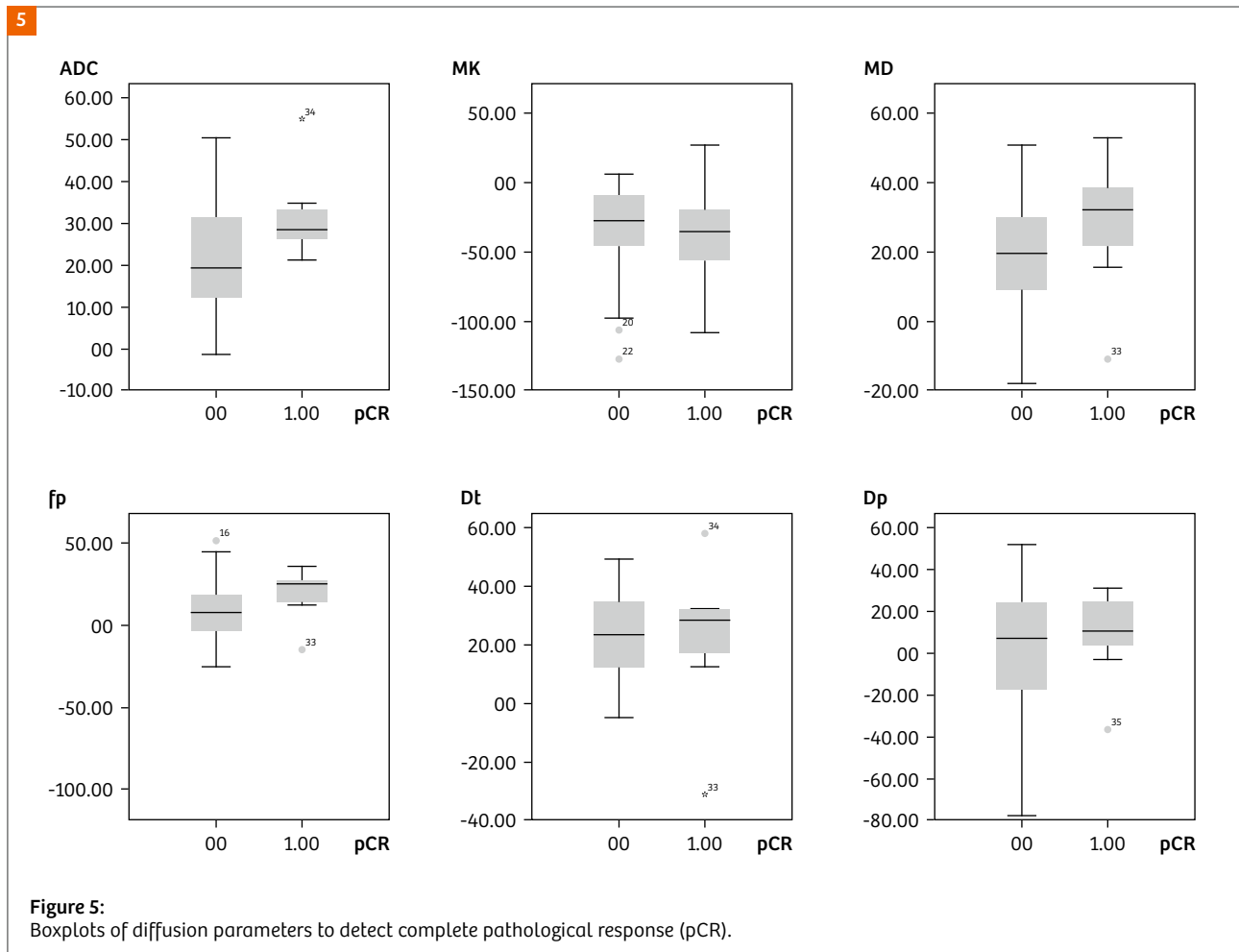
from non-responders (sensitivity 94%, specificity 84%, accuracy 89%, cut-off value = -7.8%) and the best diagnostic performance also for discriminating pCR (sensitivity 86%, specificity 89%, accuracy 89%, cut-off value = 68.2%). We also demonstrated that linearly combining each possible parameter couple or all functional IVIM-derived parameters did not increase accuracy compared to SIS alone. In this study we also extrapolated parameters derived from DKI using the Siemens Healthineers MR Body Diffusion Toolbox.

Our findings showed that, on the basis of only two MRI studies (basal and preparatory), there were statistically significant differences in ΔSIS values between responder and non-responder patients and between complete and incomplete pathological response (p << 0.01 at Mann-Whitney test) while there were no statistically significant differences in the percentage change of the parameters derived from IVIM and DKI. The best parameter for discriminating responders from non-responders and to differentiate complete from incomplete response by ROC analysis was SIS (sensitivity 94%, specificity 84%, accuracy 89%, AUC = 0.95, cut-off value = -7.8%). However, also, ΔADC showed a good diagnostic accuracy of 71% in discriminating responders from non-responders and an accuracy of 60% in differentiating complete pathological

Responders versus non-reponders

	AUC	Sensitivity	Specificity	PPV	NPV	Accuracy	Cut-off
ADC	0.67	0.88	0.58	0.64	0.85	0.71	18.63
MK	0.37	0.06	1.00	1.00	0.56	0.57	2.19
MD	0.51	0.63	0.63	0.59	0.67	0.63	18.60
fp	0.42	0.38	0.68	0.50	0.57	0.54	15.32
Dt	0.63	0.75	0.74	0.71	0.78	0.74	25.59
Dp	0.40	1.00	0.05	0.47	1.00	0.49	-79.01
SIS	0.95	0.94	0.84	0.83	0.94	0.89	-7.76

Table 3:
Diagnostic performance of each MR-derived parameter to discriminate responders from non-responders.

Abbreviations: AUC = area under ROC curve; PPV = positive predictive value; NPV = negative predictive value

Complete versus incomplete reponders

	AUC	Sensitivity	Specificity	PPV	NPV	Accuracy	Cut-off
ADC	0.73	1.00	0.50	0.33	1.00	0.60	19.11
MK	0.40	0.14	1.00	1.00	0.82	0.83	2.19
MD	0.68	0.71	0.75	0.42	0.91	0.74	25.17
fp	0.70	0.71	0.75	0.42	0.91	0.74	15.32
Dt	0.57	0.71	0.57	0.29	0.89	0.60	25.59
Dp	0.58	0.86	0.43	0.27	0.92	0.51	-11.85
SIS	0.88	0.86	0.89	0.67	0.96	0.89	-70.00

Table 4:
Diagnostic performance of each MR-derived parameter to detect complete pathological response (pCR).

Abbreviations: AUC = area under ROC curve; PPV = positive predictive value; NPV = negative predictive value

from incomplete response after SCR. For IVIM DWI derived parameters the best results to discriminate responders from non-responders were obtained with Dt (sensitivity 75%, specificity 74%, AUC = 0.63, accuracy 74%, cut-off value = 25.59%). SIS obtained the best diagnostic performance also to discriminate pCR (sensitivity 86%, specificity 89%, accuracy 89%, AUC = 0.88, cut-off value = 68.2%). A high accuracy AUC (74%) was also obtained by fp to detect pathological complete response after SCR with an area under ROC of 0.70, a sensitivity of 71%, specificity of 75%, and a cut-off value = 15.32%.

Further studies are necessary to evaluate whether combining different functional imaging techniques could increase the specificity therapy response after SCR, as already demonstrated by Lambrecht et al. [47] with the combination of ^{18}F-FDG PET/CT with pre-treatment DWI to increase the specificity of response assessment.

Some potential limitations deserve special consideration here: the MR images were evaluated based on the consensus of two radiologists in a single session for each patient so that the intra-observer variability was not assessed. A more extensive patient panel would probably strengthen the power of this study in SCR therapy assess-ment. A reproducibility analysis of MR-derived parameters was not performed, however the use of mean values for each DCE- and DW parameter, extracted by volume of interest, allows more robust measures to be obtained.

In conclusion, the Standardized Index of Shape is a promising DCE-MRI angiogenic biomarker for assessing preoperative treatment response after SCR with delayed surgery and it allows us to identify pathological complete response enabling us to direct surgery in line with tailored and conservative treatment. However, parameters derived from IVIM and DKI reflect tissue response changes and could be used to assess pathological response.
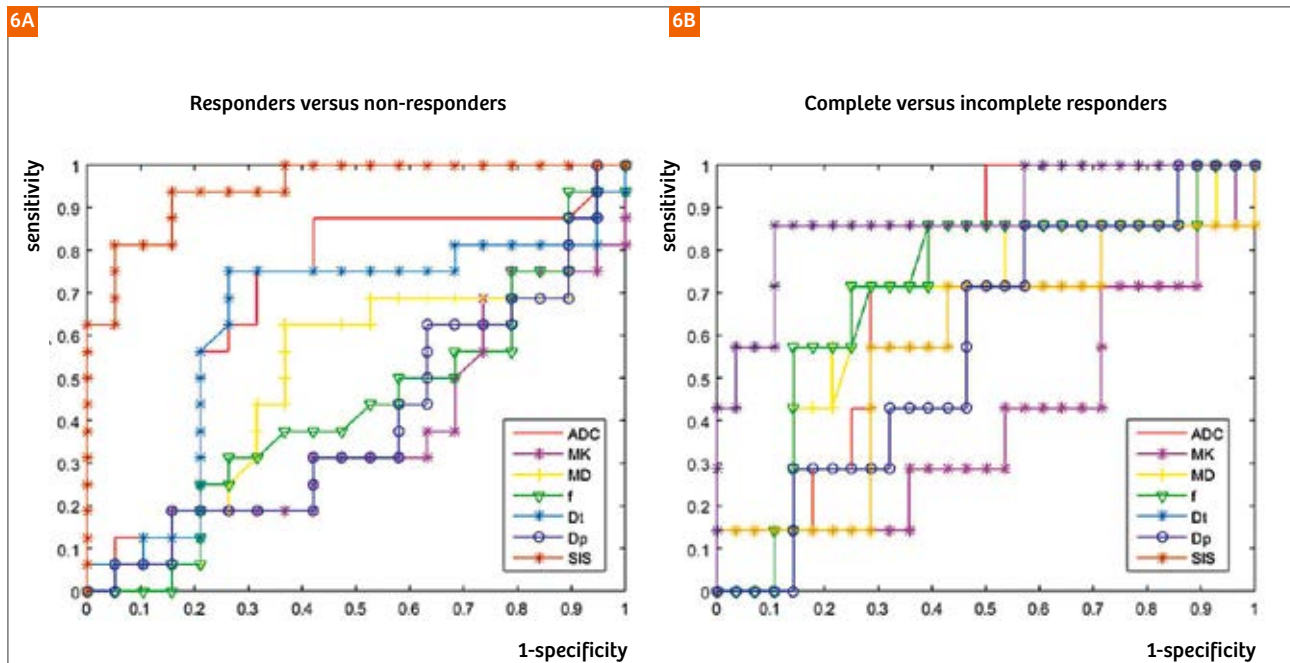
Acknowledgements

Figure 6:
ROC analysis for the best MR-derived parameters to predict pathological complete response and responder patients of SCRDS.

References

1 Avallone A, Aloj L, Delrio P, Pecori B, Leone A, Tatangelo F, Perri F, Petrillo A, Scott N, Budillon A. Multidisciplinary approach to rectal cancer: are we ready for selective treatment strategies? Anticancer Agents Med Chem. 2013 Jul 1;13(6):852-60.

2 Avallone A, Delrio P, Guida C, Tatangelo F, Petrillo A, Marone P, Cascini LG, Morrica B, Lastoria S, Parisi V, Budillon A, Comella P. Biweekly oxaliplatin,raltitrexed, 5-fluorouracil and folinic acid combination chemotherapy during preoperative radiation therapy for locally advanced rectal cancer: a phase I-II study. Br J Cancer. 2006 Jun 19;94(12):1809-15. Epub 2006 May 30.

3 Delrio P, Avallone A, Guida C, Lastoria S, Tatangelo F, Cascini GM, Marone P, Petrillo A, Budillon A, Di Marzo M, Palaia R, Albino V, De Rosa V, Parisi V. Multidisciplinary approach to locally advanced rectal cancer: results of a single institution trial. Suppl Tumori. 2005 May-Jun;4(3):8.

4 Zhou ZR, Liu SX, Zhang TS, Chen LX, Xia J, Hu ZD, Li B. Short-course preoperative radiotherapy with immediate surgery versus long-course chemoradiation with delayed surgery in the treatment of rectal cancer: a systematic review and meta-analysis. Surg Oncol. 2014 Dec;23(4):211-21.

5 Latkauskas T, Pauzas H, Gineikiene I, Janciauskiene R, Juozaityte E, Saladzinskas Z, et al. Initial results of a randomized controlled trial comparing clinical and pathological downstaging of rectal cancer after preoperative short-course radiotherapy or long-term chemoradiotherapy, both with delayed surgery. Colorectal Disease: The Official Journal of the Association of Coloproctology of Great Britain and Ireland. 2012;14(3):294–8.

6 Bujko K, Kolodziejczyk M. The 5 x 5 Gy with delayed surgery in non-resectable rectal cancer: a new treatment option. Radiotherapy and Oncology: Journal of the European Society for Therapeutic Radiology and Oncology. 2008;87(3):311–3.

7 Beppu N, Matsubara N, Noda M, Yamano T, Kakuno A, Doi H, Kamikonya N, Kimura F, Yamanaka N, Yanagi H, Tomita N. Short-course radiotherapy with delayed surgery versus conventional chemoradiotherapy: A comparison of the short- and long-term outcomes in patients with T3 rectal cancer. Surgery. 2015; 158(1):225-35.

8 Pettersson D, Holm T, Iversen H, Blomqvist L, Glimelius B, Martling A. Preoperative short-course radiotherapy with delayed surgery in primary rectal cancer. The British Journal of Surgery. 2012; 99(4):577-83.

9 Pettersson D, Lörinc E, Holm T, Iversen H, Cedermark B, Glimelius B, Martling A. Tumour regression in the randomized Stockholm III Trial of radiotherapy regimens for rectal cancer. The British Journal of Surgery. 2015; 102(8):972-8; discussion 8.

10 Radu C, Berglund A, Pahlman L, Glimelius B. Short-course preoperative radiotherapy with delayed surgery in rectal cancer – a retrospective study. Radiotherapy and Oncology: Journal of the European Society for Therapeutic Radiology and Oncology. 2008;87(3):343–9.

11 Hatfield P, Hingorani M, Radhakrishna G, Cooper R, Melcher A, Crellin A, Kwok-Williams M, Sebag-Montefiore D. Short-course radiotherapy, with elective delay prior to surgery, in patients with unresectable rectal cancer who have poor performance status or significant co-morbidity. Radiotherapy and Oncology: Journal of the European Society for Therapeutic Radiology and Oncology. 2009; 92(2):210-4.

12 Valentini V, Glimelius B, Haustermans K, Marijnen CA, Rodel C, Gambacorta MA, et al. EURECCA consensus conference highlights about rectal cancer clinical management: the radiation oncologist's expert review. Radiotherapy and Oncology: Journal of the European Society for Therapeutic Radiology and Oncology. 2014;110(1):195–8.

13 Avallone A, Piccirillo MC, Delrio P, Pecori B, Di Gennaro E, Aloj L, Tatangelo F, D'Angelo V, Granata C, Cavalcanti E, Maurea N, Maiolino P, Bianco F, Montano M, Silvestro L, Terranova Barberio M, Roca MS, Di Maio M, Marone P, Botti G, Petrillo A, Daniele G, Lastoria S, Iaffaioli VR, Romano G, Caracò C, Muto P, Gallo C, Perrone F, Budillon A. Phase 1/2 study of valproic acid

and short-course radiotherapy plus capecitabine as preoperative treatment in low-moderate risk rectal cancer-V-shoRT-R3 (Valproic acid – short Radiotherapy – rectum 3rd trial). BMC Cancer. 2014 Nov 24;14:875.

14 Heo SH, Kim JW, Shin SS, Jeong YY, Kang H-K. Multimodal imaging evaluation in staging of rectal cancer. World Journal of Gastroenterology: WJG. 2014;20(15):4244-55.

15 Fusco R, Sansone M, Petrillo M, Avallone A, Delrio P, Tatangelo F, Petrillo A. Role of Magnetic Resonance Imaging in Locally Advanced Rectal Cancer, Colorectal Cancer – Surgery, Diagnostics and Treatment, Dr. Jim Khan (ed.), InTech Available from: doi 10.5772/56831.

16 Beets-Tan RG, Beets GL. Rectal cancer: review with emphasis on MR imaging. Radiology 2004;232(2):335–346.

17 Leach MO, Brindle KM, Evelhoch JL, Griffiths JR, Horsman MR, Jackson A, Jayson GC, Judson IR, Knopp MV, Maxwell RJ, McIntyre D, Padhani AR, Price P, Rathbone R, Rustin GJ, Tofts PS, Tozer GM, Vennart W, Waterton JC, Williams SR, Workman P; Pharmacodynamic/Pharmacokinetic Technologies Advisory Committee, Drug Development Office, Cancer Research UK. The assessment of antiangiogenic and antivascular therapies in early-stage clinical trials using magnetic resonance imaging: issues and recommendations. Br J Cancer 2005;92(9):1599–610.

18 Petrillo A, Fusco R, Petrillo M, Granata V, Sansone M, Avallone A, Delrio P, Pecori B, Tatangelo F, Ciliberto G. Standardized Index of Shape (SIS): a quantitative DCE-MRI parameter to discriminate responders by non-responders after neoadjuvant therapy in LARC. Eur Radiol. 2015 Jan 11.

19 Petrillo M, Fusco R, Catalano O, Sansone M, Avallone A, Delrio P, Pecori B, Tatangelo F, Petrillo A. MRI for Assessing Response to Neoadjuvant Therapy in Locally Advanced Rectal Cancer Using DCE-MR and DW-MR Data Sets: A Preliminary Report. Biomed Res Int. 2015:514740.

20 Beets-Tan RG, Beets GL. MRI for assessing and predicting response to neoadjuvant treatment in rectal cancer. Nat Rev Gastroenterol Hepatol. 2014 Aug;11(8):480-8.

21 Phongkitkarun S, Tohmad U, Larbcharoensub N, Sumbunnanondha K, Swangsilpa T, Sirachainan E. DCE-MRI-Derived Parameters as Predictors of Response to Neo-Adjuvant Chemoradiation Treatment of Rectal Carcinoma. J Med Assoc Thai. 2016 Mar;99(3):338-47.

22 Petrillo A, Fusco R, Granata V, Setola SV, Sansone M, Rega D, Delrio P, Bianco F, Romano GM, Tatangelo F, Avallone A, Pecori B. MR imaging perfusion and diffusion analysis to assess preoperative Short Course Radiotherapy response in locally advanced rectal cancer: Standardized Index of Shape by DCE-MRI and intravoxel incoherent motion-derived parameters by DW-MRI. Med Oncol. 2017 Nov 18;34(12):198.

23 Le Bihan D, Breton E, Lallemand D, Aubin ML, Vignaud J, Laval-Jeantet M. Separation of diffusion and perfusion in intravoxel incoherent motion MR imaging. Radiology. 1988 Aug;168(2):497-505.

24 Le Bihan D, Breton E, Lallemand D, Grenier P, Cabanis E, Laval-Jeantet M. MR imaging of intravoxel incoherent motions: application to diffusion and perfusion in neurologic disorders. Radiology 1986; 161(2):401-7.

25 Oto A, Yang C, Kayhan A, Tretiakova M, Antic T, Schmid-Tannwald C, Eggener S, Karczmar GS, Stadler WM. Diffusion-weighted and dynamic contrast-enhanced MRI of prostate cancer: correlation of quantitative MR parameters with Gleason score and tumor angiogenesis. AJR Am J Roentgenol. 2011 Dec;197(6):1382-90.

26 Curvo-Semedo L, Lambregts DM, Maas M, Thywissen T, Mehsen RT, Lammering G, Beets GL, Caseiro-Alves F, Beets-Tan RG. Rectal cancer: assessment of complete response to preoperative combined radiation therapy with chemotherapy – conventional MR volumetry versus diffusion-weighted MR imaging. Radiology. 2011 Sep;260(3):734-43.

27 A, Deux J-F, Brugieres P, Rahmouni A. Liver cirrhosis: intravoxel

incoherent motion MR imaging-pilot study. Radiology 2008; 249(3): 891-9.

28 Wirestam R, Borg M, Brockstedt S, Lindgren A, Holtas S, Stahlberg F. Perfusion-related parameters in intravoxel incoherent motion MR imaging compared with CBV and CBF measured by dynamic susceptibility contrast MR technique. Acta Radiol. 2001; 42(2): 123-8.

29 Granata V, Fusco R, Catalano O, Guarino B, Granata F, Tatangelo F, Avallone A, Piccirillo M, Palaia R, Izzo F, Petrillo A. Intravoxel incoherent motion (IVIM) in diffusion-weighted imaging (DWI) for Hepatocellular carcinoma: correlation with histologic grade. Oncotarget. 2016 Nov 29;7(48):79357-64.

30 Granata V, Fusco R, Catalano O, Filice S, Amato DM, Nasti G, Avallone A, Izzo F, Petrillo A. Early Assessment of Colorectal Cancer Patients with Liver Metastases Treated with Antiangiogenic Drugs: The Role of Intravoxel Incoherent Motion in Diffusion-Weighted Imaging. PLoS One. 2015 Nov 13;10(11):e0142876.

31 Koh DM, Collins DJ, Orton MR. Intravoxel incoherent motion in body diffusion-weighted MRI: reality and challenges. AJR Am J Roentgenol 2011; 196(6): 1351–1361.

32 Jensen JH, Helpern JA. MRI quantification of non-Gaussian water diffusion by kurtosis analysis. NMR Biomed. 2010; 23:698–710.

33 Dresen RC, Beets GL, Rutten HJ, Engelen SM, Lahaye MJ, Vliegen RF, de Bruïne AP, Kessels AG, Lammering G, Beets-Tan RG. Locally advanced rectal cancer: MR imaging for restaging after neoadjuvant radiation therapy with concomitant chemotherapy. Part I. Are we able to predict tumor confined to the rectal wall? Radiology 2009;252(1):81-91.

34 SIS Tool by Antonella Petrillo available on request at an.petrillo@istitutotumori.na.it

35 Fusco R, Petrillo A, Petrillo M, Sansone M. Use of Tracer Kinetic Models for Selection of Semi-Quantitative Features for DCE-MRI Data Classification. Applied Magnetic Resonance. 2013;44(11):1311-24.

36 Andreola S, Leo E, Belli F, Bonfanti G, Sirizzotti G, Greco P, Valvo F, Tomasic G, Gallino GF. Adenocarcinoma of the lower third of the rectum surgically treated with a < 10-mm distal clearance: preliminary results in 35 N0 patients. Ann Surg Oncol 2001;8(7):611–615.

37 Mandard AM, Dalibard F, Mandard JC, Marnay J, Henry-Amar M, Petiot JF, Roussel A, Jacob JH, Segol P, Samama G, et al. Pathologic assessment of tumor regression after preoperative chemoradiotherapy of esophageal carcinoma. Clinicopathologic correlations. Cancer. 1994 Jun 1;73(11):2680-6.

38 Choi MH, Oh SN, Rha SE, Choi JI, Lee SH, Jang HS, Kim JG, Grimm R, Son Y. Diffusion-weighted imaging: Apparent diffusion coefficient histogram analysis for detecting pathologic complete response to chemoradiotherapy in locally advanced rectal cancer. J Magn Reson Imaging. 2015 Dec 15. Available from: doi: 10.1002/jmri.25117.

39 Doi H, Beppu N, Kato T, Noda M, Yanagi H, Tomita N, Kamikonya N, Hirota S. Diffusion-weighted magnetic resonance imaging for prediction of tumor response to neoadjuvant chemoradiotherapy using irinotecan plus S-1 for rectal cancer. Mol Clin Oncol. 2015 Sep;3(5):1129-34.

40 Nougaret S, Vargas HA, Lakhman Y, Sudre R, Do RK, Bibeau F, Azria D, Assenat E, Molinari N, Pierredon MA, Rouanet P, Guiu B. Intravoxel Incoherent Motion-derived Histogram Metrics for Assessment of Response after Combined Chemotherapy and Radiation Therapy in Rectal Cancer: Initial Experience and Comparison between Single-Section and Volumetric Analyses. Radiology. 2016 Aug;280(2):446-54.

41 Petrillo A, Fusco R, Petrillo M, Granata V, Delrio P, Bianco F,

Pecori B, Botti G, Tatangelo F, Caracò C, Aloj L, Avallone A, Lastoria S. Standardized Index of Shape (DCE-MRI) and Standardized Uptake Value (PET/CT): Two quantitative approaches to discriminate chemo-radiotherapy locally advanced rectal cancer responders under a functional profile. Oncotarget. 2017 Jan 31;8(5):8143-53.

42 Iima M, Le Bihan D. Clinical Intravoxel Incoherent Motion and Diffusion MR Imaging: Past, Present, and Future. Radiology. 2016 Jan;278(1):13-32.

43 Rega D, Pecori B, Scala D, Avallone A, Pace U, Petrillo A, Aloj L, Tatangelo F, Delrio P. Evaluation of Tumor Response after Short-Course Radiotherapy and Delayed Surgery for Rectal Cancer. PLoS One. 2016 Aug 22;11(8):e0160732.

44 Pecori B, Lastoria S, Caracò C, Celentani M, Tatangelo F, Avallone A, Rega D, De Palma G, Mormile M, Budillon A, Muto P, Bianco F, Aloj L, Petrillo A, Delrio P. Sequential PET/CT with [18F]-FDG Predicts Pathological Tumor Response to Preoperative Short Course Radiotherapy with Delayed Surgery in Patients with Locally Advanced Rectal Cancer Using Logistic Regression Analysis. PLoS One. 2017 Jan 6;12(1):e0169462.

45 Siegel R, Dresel S, Koswig S, Gebauer B, Hunerbein M, Schneider W, Schlag PM. Response to preoperative short-course radiotherapy in locally advanced rectal cancer: value of f-fluorodeoxyglucose positron emission tomography. Onkologie. 2008; 31(4):166-72.

46 Janssen MH, Ollers MC, van Stiphout RG, Buijsen J, van den Bogaard J, de Ruysscher D, Lambin P, Lammering G. Evaluation of early metabolic responses in rectal cancer during combined radiochemotherapy or radiotherapy alone: sequential FDG-PET-CT findings. Radiotherapy and Oncology: Journal of the European Society for Therapeutic Radiology and Oncology. 2010; 94(2):151-5.

47 Lambrecht M, Deroose C, Roels S, Vandecaveye V, Penninckx F, Sagaert X, van Cutsem E, de Keyzer F, Haustermans K. The use of FDG-PET/CT and diffusion weighted magnetic resonance imaging for response prediction before, during and after preoperative chemoradiotherapy for rectal cancer. Acta Oncol 2010;49:956–63.

· ·

Contact   Roberta Fusco
                Division of Radiology, Department of Diagnostic Imaging, Radiant and Metabolic Therapy,
                Istituto Nazionale Tumori (IRCCS) Fondazione G. Pascale

                Via Mariano Semmola 80131
                Naples
                Italy
                Phone: 00390815903738
                Fax: 00390815903825
                r.fusco@istitutotumori.na.it